Analysis and Guideline for Determining Piezoelectric Coefficient for Films With Substrate Constraint

Qinwen Xu, Jie Zhou, Shashidhara Acharya, *Member, IEEE*, Jianwei Chai, Mingsheng Zhang, Chengliang Sun, *Member, IEEE*, and Kui Yao, *Fellow, IEEE*

***Abstract*—Piezoelectric films including coatings are widely employed in various electromechanical devices. Precise measurement for piezoelectric film properties is crucial for both piezoelectric material development and design of the piezoelectric devices. However, substrate constraint on the deformation of piezoelectric films could cause significant impacts on the reliability and accuracy of the piezoelectric coefficient measurement. Through both theoretical finite element analysis (FEA) and experimental validation, here we have identified three important factors that strongly affect the measurement results: ratio of Young's modulus of substrate to piezoelectric film, ratio of electrode size to substrate thickness, and test frequency. Our investigations show that a relatively smaller substrate's Young's modulus to film, and a larger ratio of electrode size to substrate thickness would cause a larger substrate bending effect and thus potentially more significant measurement errors. Moreover, intense transversal displacement fluctuation can be excited at excessively high frequencies, leading to unreliable measurements. Various well-established piezoelectric measurement methods are compared with outstanding measurement issues identified for those commonly used piezoelectric films and substrates. We further establish the guidelines for piezoelectric coefficient measurements to achieve high reliability and accuracy, thus important to the wide technical community with interests in electromechanical active materials and devices.**

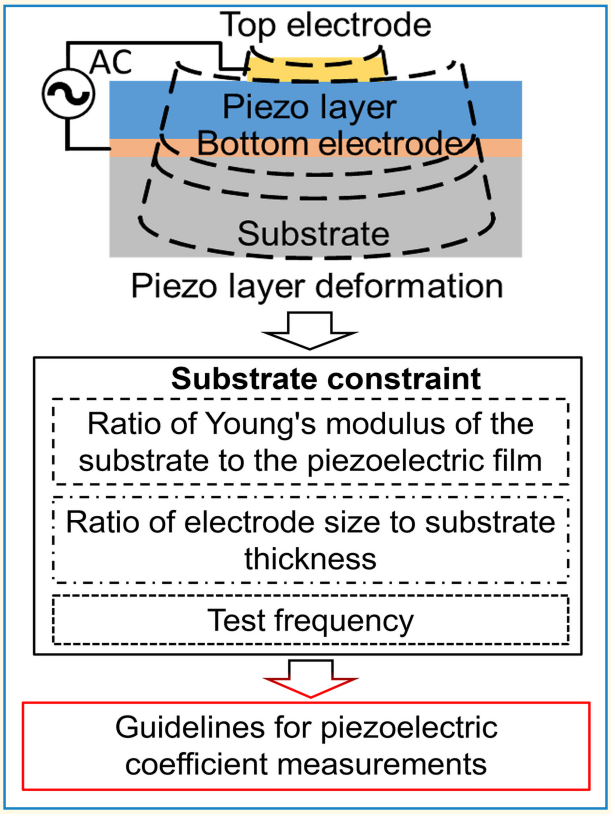

***Index Terms*—Double beam laser interferometer (DBLI), laser scanning vibrometer (LSV), piezoelectric coefficient, piezoelectric film, piezoelectric measurement.**

I. Introduction

PIEZOELECTRIC materials have been intensively studied by researchers and widely applied in many fields successfully, including biomedical applications [1], [2], [3], microfluidic control systems [4], [5], structure health monitoring [6], [7], [8], and wireless communication systems [9], [10]. With the increasingly high work frequency of devices and the requirements of device miniaturization, piezoelectric films show great application values and are successfully used in various microelectromechanical systems (MEMSs) [11], [12], [13]. To investigate piezoelectric films and their enabled electromechanical devices, it is both fundamentally and practically important to reliably determine the piezoelectric coefficients, especially the longitudinal (d_{33}) or transverse (d_{31}) piezoelectric coefficients as a commonly used basic parameter to evaluate and

Highlights

- **Establish guidelines for reliable and accurate piezoelectric coefficient measurements of films with substrates through theoretical analyses and experimental validation.**
- **Recognize three critical factors: ratio of Young's modulus of substrate to piezoelectric film, ratio of electrode size to substrate thickness, and frequency.**
- **The findings assist in accurately and reliably determining the longitudinal piezoelectric coefficient for coatings and piezoelectric films with substrates.**

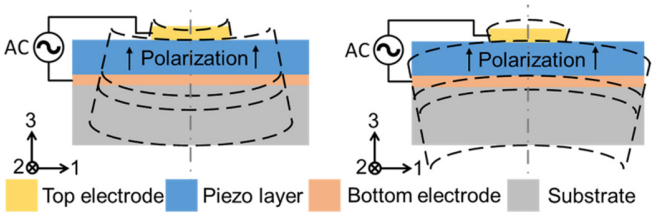

Fig. 1. Schematic illustration of distorted deformation of a piezoelectric film subjected to mechanical constraint from the substrate under an ac electric field.

compare the performance of the piezoelectric films [14], [15].

Unlike bulk piezoelectric materials, piezoelectric films usually grow on substrates, and thus cannot deform freely as the bulk material because of the substrate constraint. When an external alternating electric field is applied to the piezoelectric film, the substrate limits the deformation of the film, which causes the bending effect due to the transverse piezoelectric response [16], [17], as illustrated in Fig. 1. It is a challenge to determine piezoelectric coefficient reliably and precisely for films with substrates, including piezoelectric coatings on a mechanical structure.

In this work, to understand how to achieve a reliable d_{33} measurement for various piezoelectric films on different substrates, we systematically analyze the deformation of the film with substrate constraint taking into account three important factors, including ratio of Young's modulus of substrate to film, ratio of top electrode size to substrate thickness, and test frequency. Based on our theoretical analysis and experimental validation, we further establish the guidelines for piezoelectric coefficient measurements to achieve high reliability and accuracy, thus important to the wide technical community with interests in electromechanical active materials and devices.

II. Methods Comparison, Simulations, and Experiments

Several techniques are used to measure d_{33} of piezoelectric materials. These techniques can be divided into two main categories: 1) one utilizes the direct piezoelectric effect based on charge measurement under mechanical input like the Berlincourt method; and 2) the other utilizes the converse piezoelectric effect based on the strain measurement under an electric field like laser interferometer, laser scanning vibrometer (LSV), and piezoelectric force microscopy (PFM). The schematics of the four main test techniques are illustrated in Fig. 2. In the Berlincourt method, the system collects the charges developed in the sample under testing and the reference sample under the same mechanical load as illustrated

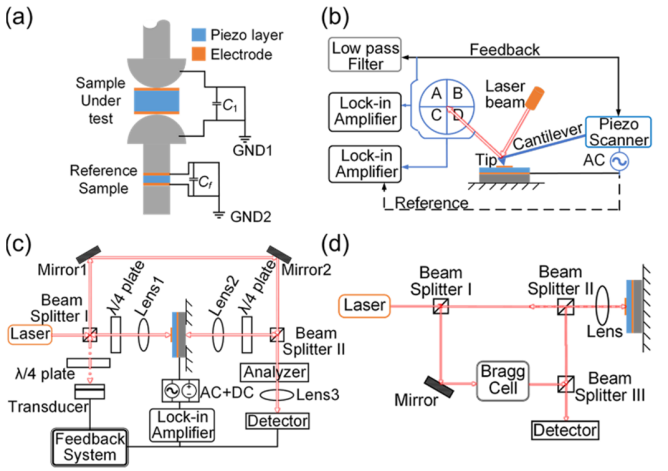

Fig. 2. Schematics of (a) Berlincourt, (b) PFM, (c) DBLI, and (d) LSV, methods for measuring piezoelectric films.

in Fig. 2(a). The d_{33} can be obtained from the ratio of the charge developed in the sample under test to the charge from [18]. The Berlincourt method is widely applied to bulk piezoelectric materials, but it's difficult to produce a homogeneous uniaxial stress in a film on a substrate without generating the bending effect [19].

For the PFM method, an ac signal is applied to the piezoelectric sample between the PFM tip and the bottom electrode of the sample, as shown in Fig. 2(b). The periodical vibration excited by the ac signal is transferred to the tip. The value of vibration displacement can be read by position-sensitive photodetectors and lock-in amplifiers. The d_{33} can be calculated from the measured displacement and the applied voltage amplitude [20]. The measured d_{33} by PFM is derived from a highly local single point without considering any bending effect, even grain-dependent because the radius of the tip apex is only tens of nanometers [21].

With the development of laser technology, laser interferometry has been applied to measure piezoelectric coefficients. However, the single-beam laser interferometer, which detects a single point from one side of the film, cannot detect or eliminate the potential large error caused by substrate bending and thus is not regarded as a reliable method. To address this issue, two methods are proposed: double beam laser interferometer (DBLI) and LSV method.

DBLI is an effective technique to minimize the impact of the bending effect, as shown in Fig. 2(c). Two probing laser beams simultaneously detect the displacement of the front and back sides of the sample. The d_{33} is calculated by the displacement difference between the front and back sides of the sample [22], [23], [24]. DBLI has high resolution

TABLE I

COMPARISON OF BERLINCOURT, PFM, DBLI, AND LSV METHODS FOR MEASURING PIEZOELECTRIC FILMS

Methods	Principle	Scan mode	Bending effect elimination	Reliability	Frequency range	Access to both sides	Precise alignment
Berlincourt	Direct piezoelectric effect	\	No	Low	Low	Required	\
DBIL	Converse piezoelectric effect	Single point	Yes	High	Medium	Required	Required
PFM	Converse piezoelectric effect	Single point	No	Low	Low	Not required	Not required
LSV	Converse piezoelectric effect	Area scan	Yes	High	High	Not required	Not required

and overcomes the influence of the bending effect. However, it requires the two probing laser beams must be strictly aligned during the experiment. Additionally, it only provides the displacement of a single point on the sample. When the back side of the sample is not accessible, it cannot be used.

LSV method is established to measure the d_{33} of piezoelectric thin films [19], [25], as depicted in Fig. 2(d), in which a laser beam is used to scan and measure the vibration displacement of the sample by Doppler frequency shift [25]. In contrast to single-point laser measurement, LSV can acquire the displacement distribution over a large area, including both amplitude and phase information, and thus can describe the vibration mode of the piezoelectric film. Thus, the error caused by the bending or moving of the substrate can be well identified and corrected without requiring access to the backside or precise alignment of laser beams [25].

Table I compares the advantages and disadvantages of these measurement techniques. DBLI and LSV are the two most reliable techniques to determine piezoelectric coefficients of piezoelectric films since they offer the feasibility to eliminate the significant errors caused by substrate movement. However, this does not mean one can always reliably obtain a piezoelectric coefficient using any of the methods. For example, if a sample suffers from any delamination, the displacement at the two surfaces by DBLI will not reflect the strain of the piezoelectric film. In addition, it has been noted that electrode size [26], electrode configurations [27], and boundary conditions of samples [28] could also impact the testing results, and thus finite element analysis (FEA) is useful to simulate the electromechanical responses of films to obtain the intrinsic d_{33} [29], [30]. However, these observations from individual-specific samples are not a systematical analysis on this matter and do not provide a general guideline for the measurements of piezoelectric coefficients. In the literature, the experimental data of piezoelectric coefficients of films and coatings samples measured by different methods and conditions have varied errors, and it is often difficult to make comparisons with reasonable reliability as for bulk piezoelectric material.

To systematically study the film deformation with substrate constraint, we conducted FEA to simulate the responses of piezoelectric films on substrates to the excitation of alternating electric fields. Fig. 3(a) illustrates the 3-D simulation model for our FEA. The basic 3-D model consists of a substrate,

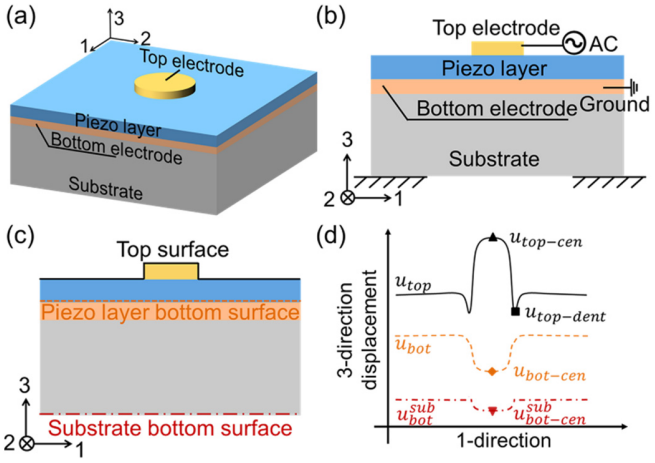

Fig. 3. (a) 3-D model built for FEA. (b) Cross-sectional view of the 3-D model in (a). (c) Three different surfaces of the sample. (d) Displacement curves of the three surfaces in (c) and the marked points of displacement curves used to calculate the measured d_{33}.

a bottom electrode, a piezoelectric film, and a circular top electrode at the center of the piezoelectric layer. Additional layers such as seed layers may be added according to specified situations. Fig. 3(b) presents a cross-sectional view of the 3-D model. AC voltage is applied to the top electrode, and the bottom electrode is grounded. Mechanical boundary conditions are rather complicated because the assumed mechanical conditions are often not fully satisfied in the experimental measurement for deformation at the level below the subnanometer in piezoelectric thin films. In all simulations, the central 6 mm-wide region of the substrate's bottom surface is set as the free boundary, while the remaining area of the substrate bottom surface is set as the fixed boundary. Although the conclusions are derived under this specific boundary condition, the comparison of results under different mechanical boundary conditions demonstrates that our findings are applicable across various boundary conditions. Detailed information on the simulation models and the comparison of results under different mechanical boundary conditions can be found in Supplementary Note 1 and Figs. S1–S3.

To simulate the influence of the relative Young's modulus of substrate to film, we use an AlN piezoelectric layer grown on sapphire substrate and vary Young's modulus of the substrate. To study the impact of the ratio of top electrode

size to substrate thickness, the top electrode diameter varies from 0.01 to 2 mm. For this study, we use three different materials—lead zirconate titanate (PZT-5H), poly(vinylidene fluoride) (PVDF), and AlN. In the simulation of the effect of test frequency, the test frequency varies from 100 Hz to 10 MHz, with AlN on sapphire as the example. All the material properties of the piezoelectric films and substrates are provided in Supplementary Note 2.

The different surfaces of the thin-film sample are shown in Fig. 3(c). Fig. 3(d) illustrates the three displacement curves obtained from the surfaces in Fig. 3(c) when the film deforms under an external electric field. u_{top} represents the displacement curve of the top surface for the sample (black solid line), u_{bot} represents the displacement curve of the bottom surface for the piezoelectric layer (yellow dashed line), and $u_{\text{bot}}^{\text{sub}}$ represents the displacement curve of the bottom surface for the substrate (red dot-dashed line). Combined with u_{top} and u_{bot}, we can get the overall dilatation deformation of the piezoelectric film as a reference. Some points at displacement curves are marked. The dent at the top surface $u_{\text{top-dent}}$ is caused by the bending effect. $u_{\text{top-cen}}$, $u_{\text{bot-cen}}$, and $u_{\text{bot-cen}}^{\text{sub}}$ represent the displacement at the center points of u_{top}, u_{bot}, and $u_{\text{bot}}^{\text{sub}}$, respectively. We can use the ratio of strain to electric field to calculate the measured d_{33} (the measured d_{33} is also called the effective longitudinal piezoelectric coefficient, $d_{33,\text{f}}$) [20].

When the film is perfectly clamped to a rigid substrate, we define this $d_{33,\text{f}}$ measured by the converse piezoelectric effect as the theoretical value (d_{33}^{C}). The d_{33}^{C} is expressed as follows [18]:

$$d_{33}^{\text{C}} = d_{33} - 2d_{31}\frac{s_{13}^{E}}{s_{11}^{E} + s_{12}^{E}} \tag{1}$$

where s_{ij}^{E} is the mechanical compliance coefficient of the piezoelectric film. Equation (1) is derived based on a polycrystalline thin film that has been poled (d_{32} equals to d_{31} because of the ceramic symmetry) [18]. However, when the values of d_{32} and d_{31} are different for the materials the d_{33}^{C} can be calculated by the following equation:

$$d_{33}^{\text{C}} = d_{33} - (d_{31} + d_{32})\frac{s_{13}^{E}}{s_{11}^{E} + s_{12}^{E}}. \tag{2}$$

The process of (2) derivation and d_{33}^{C} of AlN, PVDF, and PZT-5H can be found in Supplementary Note 3.

By using different displacement in Fig. 3(d), we define several different $d_{33,\text{f}}$ accordingly

$$d_{33}^{\text{A}} = \frac{u_{\text{top-cen}}}{V} \tag{3}$$

$$d_{33}^{\text{A-dent}} = \frac{u_{\text{top-cen}} - u_{\text{top-dent}}}{V} \tag{4}$$

$$d_{33}^{\text{F}} = \frac{u_{\text{top-cen}} - u_{\text{bot-cen}}}{V} \tag{5}$$

$$d_{33}^{\text{S}} = \frac{u_{\text{top-cen}} - u_{\text{bot-cen}}^{\text{sub}}}{V}. \tag{6}$$

Here, V is the amplitude of the ac voltage applied to the piezoelectric film. d_{33}^{A} is the apparent piezoelectric coefficient that can be obtained from single-point measurement. $d_{33}^{\text{A-dent}}$ is the piezoelectric coefficient corrected after considering the displacement of the dent, which can be measured by LSV. d_{33}^{F} is the piezoelectric coefficient deriving from the real deformation of the film but cannot be obtained directly by any experiment without removing the substrate. d_{33}^{S} is the piezoelectric coefficient combining the overall displacement of the front side of the piezoelectric film and the backside of the substrate, which can be measured by DBLI.

Among these piezoelectric coefficients, d_{33}^{A} only considers the displacement at a single point on the top surface of the piezoelectric film and is thus insufficient to mitigate any bending effect. $d_{33}^{\text{A-dent}}$ can mitigate the bending effect because the dent caused by the bending effect of the substrate has been taken into account. d_{33}^{F} is defined from the real thickness change of the piezoelectric film, it eliminates the bending effect, but it is not realistic to directly measure it. Since the displacement at the bottom of the substrate caused by the bending effect is accounted for, d_{33}^{S} can mitigate and even eliminate the bending effect in some cases. Since d_{33}^{F} is solely determined by the strain of the piezoelectric film in the thickness direction, it is the effective piezoelectric coefficient that we most desire to obtain.

When we use the LSV or DBLI method to measure the piezoelectric coefficients, we should eliminate or minimize the bending effect and its influence as much as possible to ensure the reliability of the measured data. After minimizing the influence of the bending effect, the measured $d_{33,\text{f}}$ should be as close as possible to d_{33}^{F}. However, in some situations, it may not be possible to eliminate the bending effect and to make $d_{33,\text{f}}$ close to d_{33}^{F} simultaneously. In such cases, priority should be given to eliminating or minimizing the influence of the bending effect. The numerical simulations could further substantially improve the reliability and accuracy.

To verify simulation results, we deposited a 40 nm-thick titanium nitride (TiN) layer on the 430 μm-thick commercial c-plane sapphire as the bottom electrode. Next, a 400 nm-thick AlN piezoelectric layer was deposited by magnetron sputtering on the TiN electrode in our lab. Then 80 nm-thick Au top electrodes were deposited. A stainless-steel shadow mask with different sizes of holes was used to form the circular top electrodes of different diameters. The diameters of the top circular electrodes were 0.2, 0.3, 0.4, 0.5, 0.6, 1, and 2 mm, respectively. We also used a PVDF film to verify the simulation results of the relative Young's modulus of substrate to film and the ratio of top electrode size to substrate thickness. A 28 μm-thick PVDF film was glued by conductive silver paste to a 530 μm-thick Si substrate with a Pt layer. The thicknesses of the conductive silver paste and Pt layer were 90 μm and 40 nm, respectively. The Au circular top electrodes were deposited on the PVDF film by the same top electrode deposition process as that of the AlN film. All the samples were square-shaped with a side length of 10 mm.

All the experimental samples were measured with an LSV (PSV-400, Polytec, Waldbronn, Germany) to obtain 3-D vibration modes and the displacement curves of the top surfaces for comparison with simulation results. In all measurements, we employed ac voltages identical to those used in FEA. The peripheral area of the bottom surfaces of

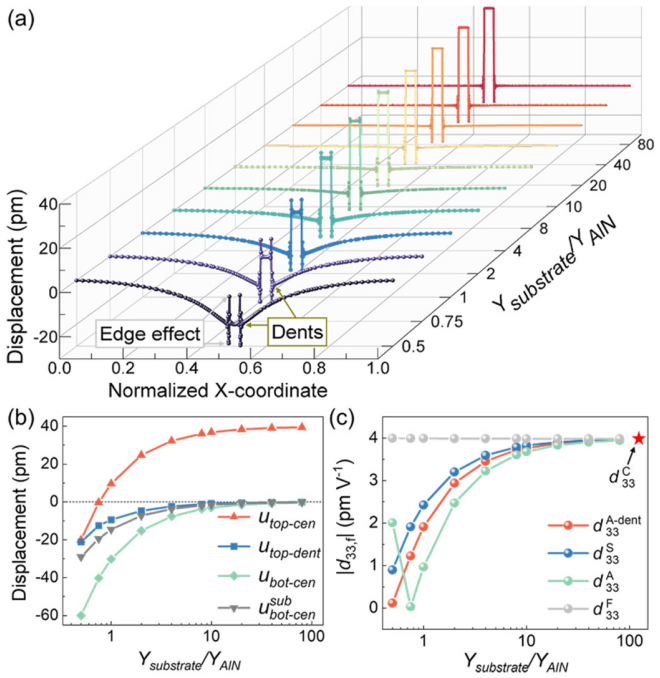

Fig. 4. (a) Displacement curves of the top surface of piezoelectric thin-film samples under different ratios of Young's modulus between the substrate and the AlN film ($Y_{substrate}/Y_{AlN}$). (b) Displacement of different points against $Y_{substrate}/Y_{AlN}$. (c) $d_{33,f}$ calculated by the displacement in (b) against $Y_{substrate}/Y_{AlN}$.

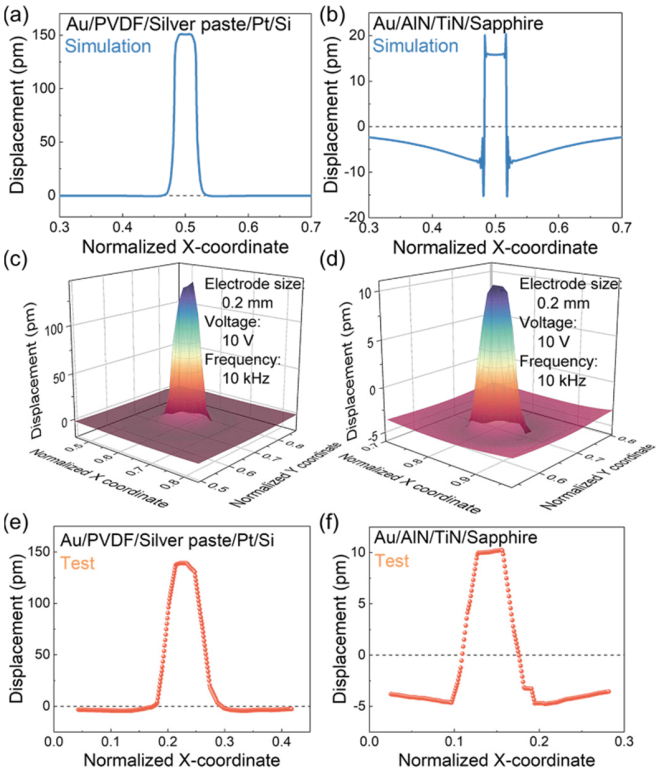

Fig. 5. Simulated top surface displacement curves of (a) PVDF film on Si substrate ($Y_{Si}/Y_{PVDF} = 69.2$) and (b) AlN film on sapphire substrate ($Y_{sapphire}/Y_{AlN} = 1.26$). Experimental top surface 3-D profiles of (c) PVDF film on Si substrate and (d) AlN film on sapphire substrate. (e) Top surface displacement curve of the PVDF film on Si substrate obtained from (c). (f) Top surface displacement curve of the AlN film on sapphire substrate obtained from (d).

all the samples was fixed to the fixture using an adhesive, as shown in Fig. S1(c). The scanning grid area covered both the top electrodes and the surrounding piezoelectric films to detect the movement caused by substrates and the deformation of the piezoelectric films simultaneously.

III. Results

Fig. 4 presents simulation results of the deformation for the piezoelectric film as a function of the ratio of Young's moduli between the substrate and piezoelectric film.

The u_{top} under various ratios of $Y_{substrate}/Y_{piezo}$ in Fig. 4(a) shows large displacement at the edge of the top electrode due to the edge effect [30]. As $Y_{substrate}/Y_{AlN}$ increases, the displacement of the dents becomes smaller, indicating that the substrate bending effect decreases. The displacement at different locations as defined in Fig. 3(d) is provided in Fig. 4(b). $u_{top\text{-}dent}$, $u_{bot\text{-}cen}$, and $u^{sub}_{bot\text{-}cen}$ converge to zero when Young's modulus of the substrate is greater than ten times of the piezoelectric layer. $u_{top\text{-}cen}$ converges to a constant (39.84 pm for the AlN film under the conditions in the simulation). The different $d_{33,f}$ values as defined in Section II are plotted in Fig. 4(c). Both $d_{33}^{A\text{-}dent}$ and d_{33}^{S} gradually increase to d_{33}^{F} with $Y_{substrate}/Y_{AlN}$ increasing. When the $Y_{substrate}/Y_{AlN}$ is greater than 10, the values of d_{33}^{A}, $d_{33}^{A\text{-}dent}$, and d_{33}^{S} approach that of d_{33}^{F}, meaning the bending effect is negligible. In this, we consider that the substrate is rigid relative to the thin film.

The hard AlN film on the sapphire substrate and soft PVDF film on the Si substrate were measured by LSV for comparison. The diameter of the top circular electrode was 0.2 mm. Fig. 5(a) and (b) present the simulation results of u_{top}. Y_{Si}/Y_{PVDF} and $Y_{Sapphire}/Y_{AlN}$ are 69.2 and 1.26, respectively. Si is much stiffer than PVDF, so the bending effect is eliminated. However, due to the proximity of Young's modulus of AlN to that of sapphire, the bending effect is nonnegligible. Hence, the displacement of the area surrounding the top electrode is substantial. 3-D profiles of the measured surface displacement for AlN on sapphire and PVDF on silicon are depicted in Fig. 5(c) and (d), respectively. The measured u_{top} corresponding to the 3-D profiles are shown in Fig. 5(e) and (f), which are consistent with the simulation results.

Fig. 6 shows the influence of the ratio of top electrode size to substrate thickness on d_{33} measurement. Here, the top electrode size refers to the diameter of the circular top electrode. The piezoelectric response for the PVDF film on Si substrate, PZT-5H film on Si substrate, AlN film on sapphire substrate, and Si substrate are simulated. When the substrate is much stiffer than the film ($Y_{substrate}/Y_{piezolayer} > 10$), $d_{33}^{A\text{-}dent}$ and d_{33}^{S} are close to d_{33}^{F} if the ratio of top electrode size to substrate thickness is greater than 2, as shown in Fig. 6(a). Nevertheless, all $d_{33,f}$ values decrease if the ratio of top electrode size to substrate thickness is less than 0.2. This is because when the deformation region is much smaller, the substrate imposes a strong constraint on the film since Young's modulus of Si is much larger than that of PVDF. For both LSV and DBLI, the ratio of top electrode size to substrate thickness should be greater than 2 when $Y_{substrate}/Y_{piezolayer} > 10$.

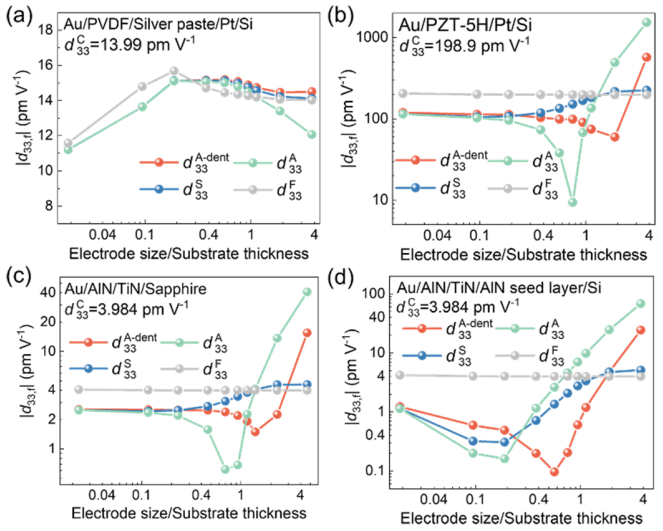

Fig. 6. $d_{33,F}$ versus the ratio of top electrode size to substrate thickness at different $Y_{substrate}/Y_{piezolayer}$. (a) PVDF film on Si substrate (Y_{Si}/Y_{PVDF} = 69.2). (b) PZT-5H film on Si substrate (($Y_{Si}/Y_{PZT\text{-}5H}$) = 2.69). (c) AlN film on sapphire substrate ($Y_{sapphire}/Y_{AlN}$ = 1.26). (d) AlN film on Si substrate (Y_{Si}/Y_{AlN} = 0.523). The curves of d_{33}^{A}, $d_{33}^{A\text{-dent}}$ and d_{33}^{S} in (a) are overlapped when the ratio of top electrode size to substrate thickness is less than 0.5. The d_{33}^{C} values of different piezoelectric films are also given in the figure.

As presented in Fig. 6(b) and (c), when the ratio of top electrode size to substrate thickness is less than 0.5 and $Y_{substrate}/Y_{piezo}$ is between 1 and 10, $d_{33}^{A\text{-dent}}$ and d_{33}^{S} are very close but lower than d_{33}^{F}. When the ratio of top electrode size to substrate thickness exceeds 0.5, both $d_{33}^{A\text{-dent}}$ and d_{33}^{A} decrease and then increase with the ratio of top electrode size to substrate thickness. Moreover, when this ratio surpasses 3, $d_{33}^{A\text{-dent}}$ and d_{33}^{A} exceeds d_{33}^{F}. d_{33}^{S} is approximately equal to d_{33}^{F} with the ratio of top electrode size to substrate thickness more than 2. When $Y_{substrate}/Y_{piezo}$ is between 1 and 10, the ratio of top electrode size to substrate thickness should be lower than 0.5 for LSV or larger than 2 for DBLI.

Fig. 6(d) illustrates the $d_{33,f}$ as a function of the ratio of top electrode size to substrate thickness when $Y_{substrate}/Y_{piezo}$ is less than 1, which is challenging to obtain accurate quantitative measurements for all the methods. When the ratio of top electrode size to substrate thickness is less than 0.2, d_{33}^{A} and d_{33}^{S} decrease as the electrode size increases. However, when the ratio of top electrode size to substrate thickness exceeds 0.2, d_{33}^{A} and d_{33}^{S} increase as the electrode size increases. For $d_{33}^{A\text{-dent}}$, this critical point of the ratio of top electrode size to substrate thickness is 0.6. d_{33}^{S} converges to d_{33}^{F} when the ratio of top electrode size to substrate thickness exceeds 2. When $Y_{substrate}/Y_{piezo}$ is less than 1, the ratio of top electrode size to substrate thickness should exceed 2 for DBLI. For LSV, to minimize the bending effect, this ratio should be less than 0.2.

Similarly, the AlN film on the sapphire and the PVDF film on the Si were measured by LSV for verification. The diameter of the top circular electrode increased from 0.2 to 2 mm. The measured 3-D profiles of the surface displacement for AlN and PVDF films with different top electrode sizes are illustrated

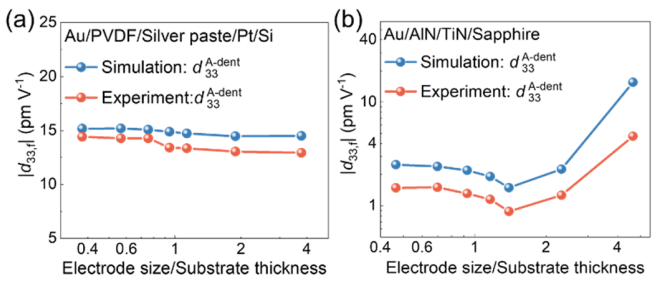

Fig. 7. Simulation $d_{33}^{A\text{-dent}}$ and experiment $d_{33}^{A\text{-dent}}$ against the ratio of top electrode size to substrate thickness of (a) PVDF film on Si substrate (Y_{Si}/Y_{PVDF} = 69.2) and (b) AlN film on sapphire substrate ($Y_{sapphire}/Y_{AlN}$ = 1.26).

in Figs. S4 and S6, respectively. The $d_{33}^{A\text{-dent}}$ was calculated through the measured displacement curves of the top surface for AlN and PVDF films shown in Figs. S5 and S7. Fig. 7 compares the $d_{33}^{A\text{-dent}}$ obtained by simulations and experiments. For both the PVDF film on Si substrate [Fig. 7(a)] and the AlN film on sapphire substrate [Fig. 7(b)], the variation trends of $d_{33}^{A\text{-dent}}$ obtained by experiments are consistent with the results obtained by simulations. The material parameters employed in simulations do not entirely match the actual material parameters, resulting in quantitative gaps in the $d_{33}^{A\text{-dent}}$ values between simulations and experiments.

The influence of test frequency on film deformation and the d_{33} measurement is depicted in Fig. 8. When the test frequency is 10 MHz, the area outside the top electrode vibrates intensely as presented in Fig. 8(a). Fig. 8(b) shows that d_{33}^{A} and $d_{33}^{A\text{-dent}}$ are much higher than d_{33}^{F} at 10 MHz, which means the results are completely unreliable. Although d_{33}^{S} is closer to d_{33}^{F} at 10 MHz, the result is still unreliable because the vibration mode is wrong for measurement (not dilation mode). The samples used in the experiment that investigated the influence of the ratio of Young's modulus of substrate to piezoelectric film were measured at different frequencies to validate the conclusions obtained from the simulation. The experiment results of $d_{33}^{A\text{-dent}}$ are compared with the simulation results in Fig. 8(c) to verify and support the simulation results (refer to measured 3-D profiles of the surface displacement at different frequencies in Fig. S8 and corresponding displacement curves in Fig. S9). $d_{33}^{A\text{-dent}}$ remains unchanged when test frequencies are lower than 10 MHz.

IV. Discussion

Since the substrate restricts the deformation of the piezoelectric film and the displacement at the bottom of the piezoelectric layer $u_{bot\text{-}cen}$ is not directly measurable, the intrinsic piezoelectric coefficient d_{33} or the d_{33}^{F} of the piezoelectric film cannot be obtained directly. Instead, the strain in the piezoelectric film always induces substrate deformation causing bending effects. This may lead to unreliable or even wrong $d_{33,f}$ measurement results in some cases. The ratio of Young's modulus of substrate to film and the ratio of electrode size to substrate thickness are recognized as the main factors that contribute to the bending effect. In addition, to achieve reliable d_{33} measurements, the mode of the deformation of the film structure should be the dilatation

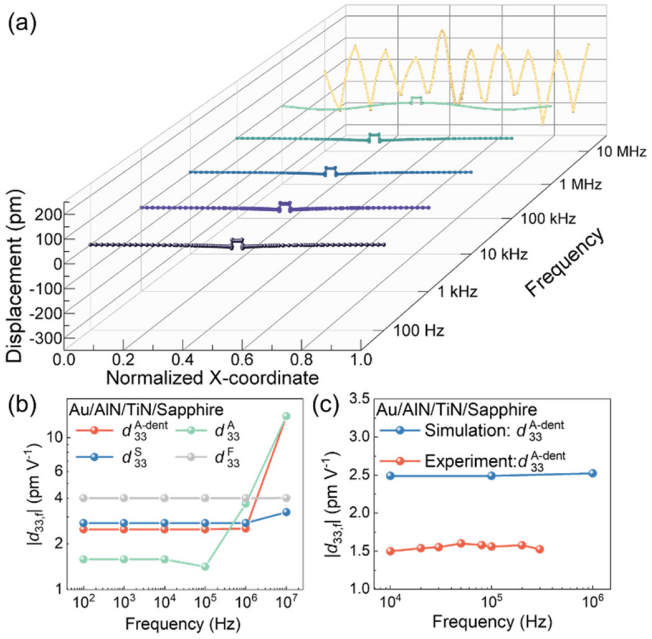

Fig. 8. (a) Simulation displacement curves of the top surface of the sample under different test frequencies. (b) Simulated $d_{33,f}$ versus the test frequency. (c) Comparison between the simulated and experimental $d_{33}^{A\text{-dent}}$ values under different test frequencies.

mode in the thickness; therefore, the test frequency is to be taken into account.

A. Ratio of Young's Modulus of Substrate to Piezoelectric Film

The vibration of piezoelectric films causes the deformation of substrates resulting in the bending effect. The larger the relative Young's modulus of substrate to film, the less prone the substrate is to deformation. As $Y_{\text{substrate}}/Y_{\text{piezo}}$ increases, the bending effect is eliminated, and all the measured $d_{33,\text{f}}$ converge to d_{33}^{F}. When $Y_{\text{substrate}}/Y_{\text{AlN}}$ is greater than 10, we consider the substrate to be rigid relative to the piezoelectric film. In this case, $d_{33}^{A\text{-dent}}$ and d_{33}^{S} are approximately equal to d_{33}^{F}.

B. Ratio of Top Electrode Size to Substrate Thickness

Generally, as the ratio of top electrode size to substrate thickness increases, the bending effect becomes more significant. However, when $Y_{\text{substrate}}/Y_{\text{piezo}}$ is greater than 10, the substrate is rigid relative to the film, and $d_{33}^{A\text{-dent}}$ and d_{33}^{S} change very slightly with the electrode size increasing. When $Y_{\text{substrate}}/Y_{\text{piezo}}$ is between 1 and 10, and the ratio of top electrode size to substrate thickness is less than 0.5, both $d_{33}^{A\text{-dent}}$ and d_{33}^{S} remain stable but substantially lower than d_{33}^{F}. When $Y_{\text{substrate}}/Y_{\text{piezo}}$ is less than 1, the smaller the ratio of top electrode size to substrate thickness, the more favorable it is for reducing the bending effect. However, regardless of $Y_{\text{substrate}}/Y_{\text{piezo}}$, when the ratio of top electrode size to substrate thickness exceeds 2, d_{33}^{S} approximates to d_{33}^{F}. This is because when the bending effect strengthens, the displacement of the bottom surface of the substrate becomes closer to the displacement of the bottom surface of the piezoelectric layer. However, in this case, the precise alignment of the double laser beams in DBLI will be critical to exclude the bending displacement from being counted as thickness dilatation, which could cause large measurement errors since the magnitude of the former is many orders of magnitude larger.

C. Test Frequency

The test cannot be conducted when any resonance frequency happens because much more significant vibration displacement occurs at resonances. In addition, the area covered with top electrodes can be considered as an elastic wave source excited by the ac electric field. The vibration of piezoelectric films simultaneously induces acoustic waves propagating along any thickness or in-plane directions. The acoustic waves propagating along an in-plane direction cause much larger transversal displacement fluctuation. The wave-induced transversal displacement fluctuation is minimal at low test frequencies but becomes significant at high frequencies (the exact frequency depends on the acoustic parameters and sample dimension). As illustrated in Fig. 8, the transversal displacement fluctuation can be observed at 1 MHz and becomes much larger at 10 MHz. d_{33} measured becomes incorrect in this case. LSV method is particularly useful in recognizing such abnormal vibration to ensure high measurement reliability.

D. Guidelines on d_{33} Measurement

For given piezoelectric film and substrate, $Y_{\text{substrate}}/Y_{\text{piezo}}$ is fixed. The ratio of top electrode size to substrate thickness can be selected to minimize the bending effect. The bending effect becomes weak as the ratio of top electrode size to substrate thickness decreases. Test frequency is another important parameter to be considered for d_{33} measurement. Taking into account the above factors and analysis outcomes, we recommend DBLI and LSV methods for quantitative d_{33} measurement with the following guidelines.

1) When the ratio of top electrode size to substrate thickness is greater than 2 and at a relatively lower frequency, d_{33}^{S} measured by DBLI is close to d_{33}^{F}, regardless of $Y_{\text{substrate}}/Y_{\text{piezo}}$. However, this requires access to both sides for the laser beams and very precise alignment of the two beams for DBLI. Because the displacement caused by the bending effect is much more significant than film dilatation, minor misalignment can result in a huge measurement error for the DBLI method.
2) LSV should be used to replace single-point laser vibrometer to measure d_{33} with acceptable reliability, because the substrate bending effect cannot be determined by single-point measurement and $d_{33}^{A\text{-dent}}$ should be used instead of d_{33}^{A} to improve the accuracy. When $Y_{\text{substrate}}/Y_{\text{piezo}}$ is greater than 10, the ratio of top electrode size to substrate thickness should be larger than 2. When $Y_{\text{substrate}}/Y_{\text{piezo}}$ is between 1 and 10, the ratio of top electrode size to substrate thickness should be below 0.5. When $Y_{\text{substrate}}/Y_{\text{piezo}}$ is less than 1, the

TABLE II
GUIDELINES ON d_{33} MEASUREMENTS FOR SEVERAL MOST IMPORTANT PIEZOELECTRIC THIN-FILM MATERIALS, BY LSV AND DBLI

Piezoelectric material	Substrate material	$Y_{substrate}/Y_{piezo}$ [a]	a = Electrode size/Substrate thickness [b]		Test frequency [d]
			LSV	DBLI [c]	
PVDF	Si	$Y_{Si}/Y_{PVDF} > 10$	$a > 2$	$a > 2$	kHz to MHz
PZT	Si	$1 < Y_{Si}/Y_{PZT} < 10$	$a < 0.5$	$a > 2$	kHz to MHz
(K,Na)NbO_3	Si	$1 < Y_{Si}/Y_{(K,Na)NbO_3} < 10$	$a < 0.5$	$a > 2$	kHz to MHz
AlN	Sapphire	$1 < Y_{Sapphire}/Y_{AlN} < 10$	$a < 0.5$	$a > 2$	kHz to MHz
AlN	Si	$Y_{Si}/Y_{AlN} < 1$	$a < 0.2$	$a > 2$	kHz to MHz

[a] The ratio of Young's modulus between substrate and piezoelectric film
[b] The ratio of top electrode size to substrate thickness
[c] Highly precise laser alignment is critical
[d] The test frequency should avoid resonance, environmental noise and be lower than the frequency where transversal displacement fluctuation becomes significant

ratio of top electrode size to substrate thickness should be below 0.2.

3) The test frequency should be selected to avoid any resonance and be lower than the frequency where any transversal displacement fluctuation becomes intensive. It seems only LSV can identify abnormal vibration because of its unique capability to determine the vibration modes of the sample over a large area. Generally, the test frequency is in the range of kilohertz–megahertz, considering the large environmental noise at lower frequencies and large transversal displacement fluctuation at higher frequencies.
4) When it is required to obtain the intrinsic piezoelectric coefficient d_{33} of the thin-film material, in some situations, we need to further analyze the experimental measurement results with numerical simulation. By adjusting the parameters used in the simulation until the simulation results match the experimental results, the material parameters used in the simulations can be considered as the intrinsic material parameters.

Table II summarizes the guidelines on d_{33} measurement for several most technologically important piezoelectric films, including AlN, PZT, PVDF, and (K, Na)NbO_3 based on the aforementioned analysis. For other piezoelectric materials and substrate materials not listed in Table II, one can identify the corresponding $Y_{\text{substrate}}/Y_{\text{piezo}}$ in Table II and set appropriate top electrode sizes to obtain a reliable $d_{33,\text{f}}$ based on the recommended measurement techniques including DBLI and LSV.

V. CONCLUSION

From theoretical FEA and experimental measurement validation, we have recognized and systematically analyzed the influence of three main factors on the quantitative measurement reliability and accuracy for determining the longitudinal piezoelectric coefficient of thin films on a substrate structure: ratio of Young's modulus between substrate and film, ratio of electrode size to substrate thickness, and test frequency. Comparing four test techniques (Berlincourt, DBLI, PFM, and LSV), LSV and DBLI methods are more capable of providing reliable quantitative d_{33} measurement results for piezoelectric films with substrate. From our investigations, we provide guidelines on d_{33} measurement by using LSV and DBLI. As Young's modulus of substrate increases, the substrate bending effect caused by the strain of piezoelectric thin films decreases, and the measured d_{33} value gradually converges to the piezoelectric coefficient derived from the real deformation of the film (d_{33}^{F}). For DBLI, the ratio of top electrode size to substrate thickness is suggested to be greater than 2. LSV can identify abnormal vibration because of its unique capability to determine the vibration modes of the sample over a large area. For LSV, the optimal selection of electrode size depends on Young's modulus ratio between substrate and piezoelectric film (see Table II). Test frequency should be selected to avoid any resonance and be lower than the frequency where significant transversal displacement fluctuation occurs. When the determination of the intrinsic piezoelectric coefficient of a piezoelectric thin-film material is necessary, we can obtain an accurate quantitative value by matching the numerical simulations with the experimental results.

REFERENCES

[1] K. Kapat, Q. T. H. Shubhra, M. Zhou, and S. Leeuwenburgh, "Piezoelectric nano-biomaterials for biomedicine and tissue regeneration," *Adv. Funct. Mater.*, vol. 30, no. 44, Oct. 2020, Art. no. 1909045, doi: 10.1002/adfm.201909045.

[2] X. Yuan, J. Shi, Y. Kang, J. Dong, Z. Pei, and X. Ji, "Piezoelectricity, pyroelectricity, and ferroelectricity in biomaterials and biomedical applications," *Adv. Mater.*, vol. 36, no. 3, Jan. 2024, Art. no. 2308726, doi: 10.1002/adma.202308726.

[3] D. Y. Park et al., "Self-powered real-time arterial pulse monitoring using ultrathin epidermal piezoelectric sensors," *Adv. Mater.*, vol. 29, no. 37, Oct. 2017, Art. no. 1702308, doi: 10.1002/adma.201702308.

[4] Y. Q. Fu et al., "Advances in piezoelectric thin films for acoustic biosensors, acoustofluidics and lab-on-chip applications," *Prog. Mater. Sci.*, vol. 89, pp. 31–91, Aug. 2017, doi: 10.1016/j.pmatsci.2017.04.006.

[5] D. J. Collins, Z. Ma, J. Han, and Y. Ai, "Continuous micro-vortex-based nanoparticle manipulation via focused surface acoustic waves," *Lab Chip*, vol. 17, no. 1, pp. 91–103, Jan. 2017, doi: 10.1039/c6lc01142j.

[6] M. Ju et al., "Piezoelectric materials and sensors for structural health monitoring: Fundamental aspects, current status, and future perspectives," *Sensors*, vol. 23, no. 1, p. 543, Jan. 2023, doi: 10.3390/s23010543.

[7] J. Yin et al., "Conformable shear mode transducers from lead-free piezoelectric ceramic coatings: An innovative ultrasonic solution for submerged structural health monitoring," *Adv. Funct. Mater.*, vol. 34, no. 32, Mar. 2024, Art. no. 2401544, doi: 10.1002/adfm.202401544.

[8] V.-K. Wong et al., "Structural health monitoring of fastener hole using ring-design direct-write piezoelectric ultrasonic transducer," *Struct. Health Monitor.*, vol. 21, no. 6, pp. 2657–2669, Feb. 2022, doi: 10.1177/14759217211073950.

[9] Y. Liu, Y. Cai, Y. Zhang, A. Tovstopyat, S. Liu, and C. Sun, "Materials, design, and characteristics of bulk acoustic wave resonator: A review," *Micromachines*, vol. 11, no. 7, p. 630, Jun. 2020, doi: 10.3390/mi11070630.

[10] G. Giribaldi, L. Colombo, P. Simeoni, and M. Rinaldi, "Compact and wideband nanoacoustic pass-band filters for future 5G and 6G cellular radios," *Nature Commun.*, vol. 15, no. 1, p. 304, Jan. 2024, doi: 10.1038/s41467-023-44038-9.

[11] I. Kanno, "Piezoelectric MEMS: Ferroelectric thin films for MEMS applications," *Japanese J. Appl. Phys.*, vol. 57, no. 4, Mar. 2018, Art. no. 040101, doi: 10.7567/jjap.57.040101.

[12] P. Muralt, "Recent progress in materials issues for piezoelectric MEMS," *J. Amer. Ceram. Soc.*, vol. 91, no. 5, pp. 1385–1396, May 2008, doi: 10.1111/j.1551-2916.2008.02421.x.

[13] G. Pillai, A. A. Zope, J. M.-L. Tsai, and S.-S. Li, "Piezoelectric MEMS resonators: A review," *IEEE Sensors J.*, vol. 21, no. 11, pp. 12589–12605, Jun. 2021, doi: 10.1109/JSEN.2021.3073505.

[14] J.-M. Liu, B. Pan, H. L. W. Chan, S. N. Zhu, Y. Y. Zhu, and Z. G. Liu, "Piezoelectric coefficient measurement of piezoelectric thin films: An overview," *Mater. Chem. Phys.*, vol. 75, nos. 1–3, pp. 12–18, Apr. 2002, doi: 10.1016/s0254-0584(02)00023-8.

[15] J. Fialka and P. Beneš, "Comparison of methods for the measurement of piezoelectric coefficients," *IEEE Trans. Instrum. Meas.*, vol. 62, no. 5, pp. 1047–1057, May 2013, doi: 10.1109/TIM.2012.2234576.

[16] X. Yan, W. Ren, H. Xin, P. Shi, X. Chen, and X. Wu, "Influence of substrate deformation on piezoelectric displacement measurement of piezoelectric film," *Ceram. Int.*, vol. 39, pp. S583–S586, May 2013, doi: 10.1016/j.ceramint.2012.10.140.

[17] Z. Wang and J. Miao, "Critical electrode size in measurement of d_{33} coefficient of films via spatial distribution of piezoelectric displacement," *J. Phys. D, Appl. Phys.*, vol. 41, no. 3, Jan. 2008, Art. no. 035306, doi: 10.1088/0022-3727/41/3/035306.

[18] K. Lefki and G. J. M. Dormans, "Measurement of piezoelectric coefficients of ferroelectric thin films," *J. Appl. Phys.*, vol. 76, no. 3, pp. 1764–1767, Aug. 1994, doi: 10.1063/1.357693.

[19] K. Yao and F. E. H. Tay, "Measurement of longitudinal piezoelectric coefficient of thin films by a laser-scanning vibrometer," *IEEE Trans. Ultrason., Ferroelectr., Freq. Control*, vol. 50, no. 2, pp. 113–116, Feb. 2003, doi: 10.1109/TUFFC.2003.1182115.

[20] M. G. Cain, *Characterisation of Ferroelectric Bulk Materials and Thin Films*, vol. 2. Dordrecht, The Netherlands: Springer, 2014.

[21] Z. Huang et al., "Determination of piezoelectric coefficients and elastic constant of thin films by laser scanning vibrometry techniques," *Sens. Actuators A, Phys.*, vol. 135, no. 2, pp. 660–665, Apr. 2007, doi: 10.1016/j.sna.2006.10.002.

[22] A. L. Kholkin, C. Wütchrich, D. V. Taylor, and N. Setter, "Interferometric measurements of electric field-induced displacements in piezoelectric thin films," *Rev. Sci. Instrum.*, vol. 67, no. 5, pp. 1935–1941, May 1996, doi: 10.1063/1.1147000.

[23] Q. M. Zhang, W. Y. Pan, and L. E. Cross, "Laser interferometer for the study of piezoelectric and electrostrictive strains," *J. Appl. Phys.*, vol. 63, no. 8, pp. 2492–2496, Apr. 1988, doi: 10.1063/1.341027.

[24] W. Y. Pan and L. E. Cross, "A sensitive double beam laser interferometer for studying high-frequency piezoelectric and electrostrictive strains," *Rev. Sci. Instrum.*, vol. 60, no. 8, pp. 2701–2705, Aug. 1989, doi: 10.1063/1.1140644.

[25] K. Yao, S. Shannigrahi, and F. E. H. Tay, "Characterisation of piezoelectric thin films by areal laser scanning," *Sens. Actuators A, Phys.*, vol. 112, no. 1, pp. 127–133, Apr. 2004, doi: 10.1016/j.sna.2003.12.014.

[26] S. Sivaramakrishnan, P. Mardilovich, A. Mason, A. Roelofs, T. Schmitz-Kempen, and S. Tiedke, "Electrode size dependence of piezoelectric response of lead zirconate titanate thin films measured by double beam laser interferometry," *Appl. Phys. Lett.*, vol. 103, no. 13, Sep. 2013, Art. no. 132904, doi: 10.1063/1.4821948.

[27] P. M. Mayrhofer, H. Euchner, A. Bittner, and U. Schmid, "Circular test structure for the determination of piezoelectric constants of $Sc_xAl_{1-x}N$ thin films applying laser Doppler vibrometry and FEM simulations," *Sens. Actuators A, Phys.*, vol. 222, pp. 301–308, Feb. 2015, doi: 10.1016/j.sna.2014.10.024.

[28] M. Stewart et al., "Electrode size and boundary condition independent measurement of the effective piezoelectric coefficient of thin films," *APL Mater.*, vol. 3, no. 2, Feb. 2015, Art. no. 026103, doi: 10.1063/1.4907954.

[29] J. Hernando, J. L. Sánchez-Rojas, S. González-Castilla, E. Iborra, A. Ababneh, and U. Schmid, "Simulation and laser vibrometry characterization of piezoelectric AlN thin films," *J. Appl. Phys.*, vol. 104, no. 5, Sep. 2008, Art. no. 053502, doi: 10.1063/1.2957081.

[30] C. Stoeckel, C. Kaufmann, R. Schulze, D. Billep, and T. Gessner, "Precise determination of piezoelectric longitudinal charge coefficients for piezoelectric thin films assisted by finite element modeling," in *Proc. Joint IEEE Int. Symp. Appl. Ferroelectric Workshop Piezoresponse Force Microsc. (ISAF/PFM)*, Prague, Czech Republic, Jul. 2013, pp. 194–196, doi: 10.1109/ISAF.2013.6748725.

Qinwen Xu received the B.E. degree in mechanical design, manufacturing, and automation from the School of Power and Mechanical Engineering, Wuhan University, Wuhan, China, in 2019, where he is currently pursuing the Ph.D. degree in mechatronic engineering from the Institute of Technological Sciences.

His current research interests include thin film deposition, design and manufacture of radio frequency (RF) acoustic filters, and acoustic sensors.

Jie Zhou received the B.E. degree in mechanical design, manufacturing, and automation from the School of Power and Mechanical Engineering, Wuhan University, Wuhan, China, in 2018, and the Ph.D. degree in mechatronic engineering from the Institute of Technological Sciences, Wuhan University, in 2023.

From 2021 to 2022, he was a Ph.D. Exchange Scholar at the Institute of Materials Research and Engineering (IMRE), Agency for Science, Technology and Research (A*STAR), Singapore. He is currently a Thin-Film Bulk Acoustic Resonator (FBAR) Design Engineer at MEMSONICS SRC PTE. LTD., Singapore, Research and Development Center, Singapore, a position he has held since 2023. His research focuses on radio frequency (RF) resonators, filters, and sensor chips based on lamb waves.

Shashidhara Acharya (Member, IEEE) received the M.Sc. degree in materials science from Mangalore University, Mangaluru, India, in 2007, and the Ph.D. degree from the National Institute of Technology at Karnataka, Surathkal, India, in 2016.

From 2007 to 2010, he was a Project Assistant at the Department of Surface Engineering, National Aerospace Laboratories, Bengaluru. From 2017 to 2021, he was a Research Associate at the Jawaharlal Nehru Centre for Advanced Scientific Research, Bengaluru. He is currently a Senior Scientist at the Institute of Materials Research and Engineering, Singapore. His research focuses on the growth of piezoelectric and ferroelectric thin films, investigating their structure–property relationships using various analytical and spectroscopic techniques, and piezo-MEMS-based actuators and sensors.

Jianwei Chai is a Lead Research Engineer at the Institute of Materials Research and Engineering, Agency for Science, Technology and Research (A*STAR), Singapore. His research focuses on the growth of thin and ultrathin dielectric, piezoelectric, and ferroelectric films, including their compositional and structural characterizations, and their applications in ultrasonic and remote-control actuators and photoacoustic devices.

Mingsheng Zhang received the B.S. degree in applied physics, the M.S. degree in electrical materials and devices, and the Ph.D. degree in materials engineering from Shanghai Jiao Tong University, Shanghai, China, in 1988, 1991, and 1998, respectively.

Since 2000, he has been with the Agency for Science, Technology, and Research, Singapore, progressing from Research Engineer to Principal Scientist. His research interests include piezoelectric and ferroelectric materials and devices, data storage, surface characterization of materials, and MEMS.

Dr. Zhang was a recipient of the National Technology Award of Singapore in 2005.

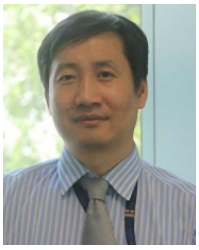

Chengliang Sun (Member, IEEE) received the B.S. and Ph.D. degrees in physics from Wuhan University, Wuhan, China, in 1999 and 2006, respectively.

From September 2004 to May 2011, he was a Research Associate at The Hong Kong Polytechnic University, Hong Kong; a Postdoctoral Associate at the University of Pittsburgh, Pittsburgh, PA, USA; and a Research Fellow at the University of Wisconsin–Madison, Madison, WI, USA. In May 2011, he joined the Institute of Microelectronics, Agency for Science, Technology and Research, Singapore, where he was a Principal Investigator. In September 2017, he joined the Institute of Technological Sciences, Wuhan University, as a Professor. His current research interests include RF resonators and filters, SAW/BAW/MEMS sensors, and ultrasound transducers.

Kui Yao (Fellow, IEEE) is currently a Senior Principal Scientist at the Institute of Materials Research and Engineering, Agency for Science, Technology and Research (A*STAR), Singapore. His research areas cover dielectric, piezoelectric, and ferroelectric materials, and the sensors and transducers enabled by these materials, including their applications for structural and condition monitoring, health care, ultrasonic and photoacoustic detection and diagnosis, noise, and vibration mitigation.